PTEN Phosphatase Selectively Binds Phosphoinositides and Undergoes Structural Changes[†]

Roberta E. Redfern,[‡] Duane Redfern,[‡] Melonnie L. M. Furgason,[§] Mary Munson,[§] Alonzo H. Ross,[§] and Arne Gericke*,[‡]

Chemistry Department, Kent State University, Kent, Ohio 44242, and Department of Biochemistry and Molecular Pharmacology, University of Massachusetts Medical School, Worcester, Massachusetts 01605

ABSTRACT: PTEN (phosphatase and tensin homologue deleted on chromosome 10) is a tumor suppressor that is mutated or deleted in a variety of human tumors, and even loss of only one PTEN gene profoundly affects carcinogenesis. PTEN encodes a phosphatidylinositol phosphate phosphatase specific for the 3-position of the inositol ring. Despite its importance, we are just beginning to understand the regulatory circuits that maintain the correct levels of PTEN phosphatase activity. Several independent studies reported that $PI(4,5)P_2$ enhances PTEN phosphatase activity, but the reasons for this enhancement are currently being debated. In this study, PTEN bound to $PI(4,5)P_2$-bearing vesicles has increased α-helicity, providing direct spectroscopic proof of a conformational change. Neither $PI(3,5)P_2$ nor $PI(3,4,5)P_3$ induced this conformational change. On the basis of experiments with two mutant PTEN proteins, it is shown that $PI(4,5)P_2$ induces this conformational change by binding to the PTEN N-terminal domain. Using PTEN protein and a 21-amino acid peptide based on the PTEN N-terminus, we tested all natural phosphatidylinositol phosphates and found preferential binding of $PI(4,5)P_2$. PTEN also binds to phosphatidylserine-bearing vesicles, resulting in a slight increase in β-sheet content. In addition, PTEN binds synergistically to $PI(4,5)P_2$ and phosphatidylserine, and hence, these anionic lipids do not compete for PTEN binding sites. Collectively, these results demonstrate that PTEN binds to membranes through multiple sites, but only $PI(4,5)P_2$ binding to the N-terminal domain triggers a conformational change with increased α-helicity.

PTEN[1] (phosphatase and tensin homologue deleted on chromosome 10) is a phosphatidylinositol phosphate (PIP) phosphatase specific for the 3-position of the inositol ring (*1*). Although PTEN shows activity toward PI(3)P, PI(3,4)-P_2, and $PI(3,4,5)P_3$, it is likely that $PI(3,4,5)P_3$ is the most important substrate in vivo (*2*). $PI(3,4,5)P_3$ affects a large variety of physiological processes by binding to signaling proteins, particularly those with a pleckstrin homology (PH) domain. Most importantly, $PI(3,4,5)P_3$ promotes cell proliferation and survival by inducing phosphorylation and activation of the Akt kinase (*3, 4*). As a result, PTEN influences

many biological processes in both developing and adult organisms (*5, 6*). PTEN is also involved in pathological processes and is deleted or inactivated in many tumor types (*7*). The frequency of tumor-associated mutations rivals that of the p53 tumor suppressor.

PTEN's structure consists of a short N-terminal PI(4,5)-P_2-binding domain, a phosphatase domain rich in α-helix, a C2 domain dominated by β-sheet, and a C-terminal tail with several phosphorylation sites (*8*). The C2 domain stabilizes the phosphatase domain through several interdomain contacts and aids the targeting of the protein to the bilayer−water interface by Ca^{2+}-independent binding to phosphatidylserine (PS). PTEN is an interfacial enzyme that is released from the membrane after hydrolyzing a few $PI(3,4,5)P_3$ molecules and then jumps to a new site; i.e., it can be considered a hopping enzyme with limited scooting ability (*9, 10*). PTEN binds to pure phosphatidylcholine vesicles (*8*) but shows a preference for negatively charged membranes (*9, 11*). Mutational analysis of PTEN suggests that both the phosphatase and the C2 domains play pivotal roles in the membrane binding event (*11, 12*). High salt concentrations inhibit PTEN binding, indicating that electrostatic forces are important for PTEN−membrane interactions (*11*). In addition, physiological salt concentrations significantly inhibited PTEN's phosphatase activity against soluble substrates like $Ins(1,3,4,5)P_4$, possibly due to altered electrostatic interactions between the positively charged residues in PTEN's active site and the substrate. In contrast, PTEN's phosphatase

activity toward lipid substrates [e.g., PI(3,4,5)P$_3$ in a lipid vesicle] was enhanced by physiological salt concentrations (*9*). The analysis of such data is complex because the univalent salt concentration strongly affects the charge of phosphoinositide headgroups (*13*), which impacts phosphoinositide−phosphoinositide interactions (*14*, *15*) and most likely the accessibility of the PI(3,4,5)P$_3$ headgroup for interfacial enzymes such as PTEN.

Several independent studies reported that PI(4,5)P$_2$ enhances PTEN phosphatase activity (*9*, *16*), but the reasons for this enhancement are currently being debated. Downes and co-workers (*9*, *17*) proposed that PTEN binds PI(4,5)P$_2$ and, thereby, place the phosphatase domain proximal to the substrate, PI(3,4,5)P$_3$. In contrast to the lipid substrates, they observed that the extent of Ins(1,3,4,5)P$_4$ hydrolysis is reduced in the presence of membrane resident PI(4,5)P$_2$, which suggests that association of PTEN with the lipid bilayer blocks access of soluble substrates to the active site. On the basis of kinetic analysis of phosphatase activity, the Ross lab proposed that in addition, PI(4,5)P$_2$ activates the phosphatase domain by inducing a conformational change (*16*). The Devreotes group suggested that PTEN's N-terminus blocks the active site, while binding to PI(4,5)P$_2$ results in a conformational change that reverses the block of the phosphatase site (*18*). In contrast, Walker et al. concluded, on the basis of their kinetic studies, that the enhancement could be best explained by membrane tethering without a conformational change (*17*). It is also possible that the conformational change upon membrane association results in enhanced specificity for lipid substrates and decreased specificity for soluble substrates like Ins(1,3,4,5)P$_4$. For myotubularin, a PTEN-related phosphatase specific for the 3-position of PI(3)P and PI(3,5)P$_2$ (*19*), a related model has been proposed. Binding of PI(5)P triggers a conformational change, which results in oligomerization and activation of the enzyme. It is intriguing that like PTEN, one of its products, PI(5)P, activates myotubularin. Despite the importance of these phosphatases to normal and pathological processes, the mechanism by which interactions with anionic lipid bilayers lead to structural changes and phosphatase activation has not been delineated.

In this study, we reach three conclusions. First, we provide spectroscopic proof that PI(4,5)P$_2$ induces a conformational change for PTEN, thereby resolving the current controversy (*9*, *10*, *16*). Second, we find that this conformational change is specifically induced by PI(4,5)P$_2$. This result contrasts with the recent proposal that the interaction of PTEN's N-terminal domain with phosphoinositides is purely nonspecific electrostatic and does not depend on which sites of the inositol ring are phosphorylated (*20*). Third, we find that PTEN binds synergistically to PI(4,5)P$_2$ and PS, and hence, these anionic lipids do not compete for binding sites. Furthermore, the effects of PI(4,5)P$_2$ and PS on the conformation of PTEN are distinct as judged by infrared spectroscopy.

MATERIALS AND METHODS

1-Palmitoyl-2-oleoylphosphatidylcholine (POPC), 1-palmitoyl-2-oleoylphosphatidylserine (POPS), brain phosphatidylinositol 4,5-bisphosphate, brain phosphatidylinositol 4-phosphate, 1-stearoyl-2-arachidonoyl 3,5-bisphosphate, and 1,2-dioleoyl-*sn*-glycerol-3-phosphoethanolamine-*N*-(1-

pyrenesulfonyl) (excitation at 347 nm, emission at 379 nm) (pyrene-labeled DOPE) were purchased from Avanti Polar Lipids (Alabaster, AL). 1-Stearoyl-2-arachidonoylphosphatidylinositol 3,4,5-trisphosphate was purchased from Cayman Chemical (Ann Arbor, MI), while all C6-BODIPY TMR-labeled phosphoinositides (excitation at 542 nm, emission at 574 nm) were purchased from Echelon Biosciences Inc. (Salt Lake City, UT). All buffers (HEPES and Tris) were of enzyme grade quality, as were EDTA, NaCl, and DTT (Fisher Scientific, Chigaco, IL). Buffers used for all fluorescence experiments were composed of 100 mM NaCl, 10 mM HEPES, and 0.1 mM EDTA (pH 7.0). The buffer used for the infrared experiments consisted of 100 mM NaCl, 10 mM Tris, and 10 mM DTT. These salts were dissolved in D$_2$O (99.9% deuterium, Fisher Scientific) and brought to pH 7.0 using DCl and NaOD. Chloroform and methanol used for preparing lipid samples were ACS grade, while the water used for these buffers was HPLC grade (Fisher Scientific). The peptide PTEN$_{1-21}$ that includes the N-terminal PI(4,5)-P$_2$-binding domain was purchased from GenScript Corp. (Scotch Plains, NJ). The purity is >99%. Mass spectra were taken to ensure the quality of the peptide. Earlier attempts to use the shorter PTEN$_{1-16}$ peptide failed because the peptide aggregated strongly.

Preparation of Recombinant PTEN. The cDNA encoding full-length (1−403) human PTEN was cloned into the *Nde*I and *Xho*I sites of the pET30b vector (Novagen), thereby introducing a six-histidine tag at the C-terminus. Point mutations were introduced with the Quick-Change site-directed mutagenesis kit from Stratagene. Deletion mutant 16−403 was prepared by PCR with the Phusion DNA polymerase (New England Biolabs). The 5′ primer included an *Nde*I restriction site and a Met initiation codon. The 3′ primer included an *Xho*I site. The PCR product was blunt end cloned into the *Eco*RV site of the pcDNA3 plasmid. This insert was released from the pcDNA3 plasmid and cloned into the *Nde*I and *Xho*I sites of pET30b.

PTEN proteins were expressed in *Escherichia coli* BL21-(DE3) cells. To increase protein solubility, cells were grown at 37 °C until the OD at 560 nm reached 0.5−0.6. The culture was shifted to 21 °C, and after 30 min, protein expression was induced with 0.05 mM isopropyl *β*-D-thiogalactoside. After 20−22 h, the culture was harvested. His$_6$ proteins were purified with a HisTrap HP kit from GE Healthcare using buffers with 10 mM mercaptoethanol. The PTEN proteins were further purified with a Superdex 200 16/60 column in 100 mM NaCl, 10 mM Tris (pH 7.4), and 1 mM dithiothreitol. The final purification was done with a MonoQ 5/5 anion exchange column in 10 mM Tris (pH 7.4) with a linear gradient from 50 to 600 mM NaCl. Fractions were analyzed by SDS−PAGE and Coomassie Blue staining. Those fractions containing >95% pure protein were pooled. Dithiothreitol was added to a concentration of 10 mM, and the proteins were stored on ice because initial experiments revealed that freezing and thawing resulted in protein aggregation. The yield of recombinant protein was 1.5−2.0 mg/mL. Phosphatase activity was confirmed as described previously (*16*).

Sample Preparation. Lipid stock solutions were dissolved in mixtures of chloroform and methanol (3:1, v/v) and stored in amber glass vials to protect them from UV light. Large unilamellar vesicles were prepared by drying lipid solutions

at ~50 °C under a stream of nitrogen to produce a lipid film. The samples were then kept overnight at ~45 °C in high vacuum to remove any residual solvent. The lipid films were resuspended in buffer solution and vortexed for 60 s three times, waiting approximately 5 min between vortexing cycles. The resulting multilamellar vesicles were then extruded through a polycarbonate film with a 100 nm pore size (Avestin, Ottawa, ON). The resulting unilamellar vesicles were checked using dynamic light scattering (HPPS and Nanosizer, Malvern Instruments, Southborough, MA) before and after experiments. Typically, these unilamellar vesicles exhibited a narrow size distribution centered at a diameter of ~112 nm. The size of the unilamellar vesicles remained unchanged during the experiments; i.e., vesicle fusion, which would unfavorably affect our fluorescence quenching experiments, did not occur.

Fluorescence Quenching Experiments Using BODIPY TMR-Labeled Phosphoinositides. Fluorescence experiments were carried out with a Varian (Walnut Creek, CA) Eclipse fluorescence spectrometer equipped with a temperature-controlled sample holder. Unilamellar mixed vesicles [99.9% POPC and 0.1% BODIPY TMR-PI(x,y)P$_2$] were made as described above, resulting in a final total lipid concentration of 0.23 mM. Half of the fluorescently labeled lipid is located on the inside of the unilamellar vesicles and, therefore, is inaccessible for the protein. These unilamellar vesicles were titrated at 20 °C with protein or peptide in 40 titration steps, reaching a protein to (outer leaflet) anionic lipid molar ratio of 0.5. The fluorescence of the BODIPY TMR probe (excitation at 542 nm, emission at 574 nm) was recorded after each addition of PTEN protein. These values were normalized to the initial fluorescence value in the absence of protein, which was set to 100%. The fluorescence intensities were then corrected for dilution.

Tryptophan Quenching Experiments. Using a Varian Eclipse spectrometer, the tryptophan fluorescence spectra of 1.5 μM protein solutions in pH 7.0 HEPES buffer (10 mM HEPES, 100 mM NaCl, and 0.1 mM EDTA) were recorded at 20 °C, using an excitation wavelength of 290 nm and scanning the emission wavelength from 300 to 380 nm. The maximum intensity value of the tryptophan emission band was recorded, and unilamellar vesicles prepared as described above were then titrated into the solution in 20 steps, until a total of 1 mM lipid had been added. The composition of the lipid vesicles varied; experiments were carried out using 97 mol % POPC and 1 mol % brain PI(4,5)P$_2$, 93 mol % POPC and 5 mol % brain PI(4,5)P$_2$, and 88 mol % POPC and 10 mol % brain PI(4,5)P$_2$. All vesicle mixtures also contained 2 mol % pyrene-labeled DOPE. The maximum intensities of the tryptophan fluorescence spectra were recorded and corrected for dilution of fluorescence as well as changes in fluorescence due to the phosphoinositide binding. The latter correction was made using vesicles lacking pyrene-labeled PE. They were then normalized to the initial value, which was set at 100%. All of these experiments were repeated at least three times. The fluorescence quenching data shown in Figures 1 and 2 were fitted with a simple binding model, $y = (K_a[\text{lipid}])/(1 + K_a[\text{lipid}])$, based on the total lipid concentration (i.e., PC + anionic lipid). In the case of strong binding to the vesicles containing PI(4,5)P$_2$ or high concentrations of PS, we made the assumption that binding was primarily due to the anionic
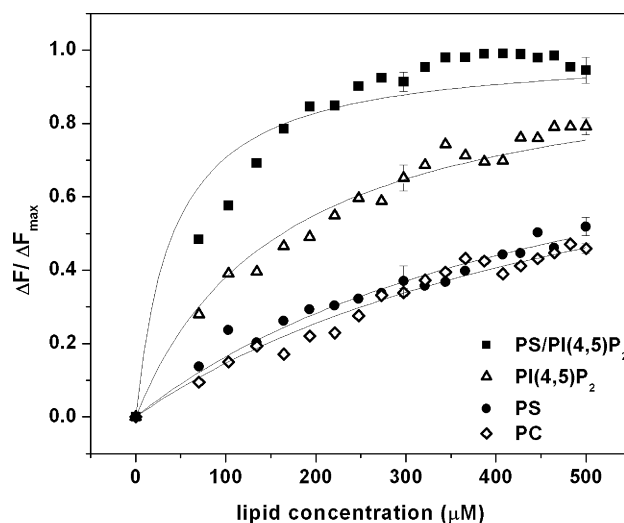

FIGURE 1: Binding of PTEN to mixed lipid vesicles. Tryptophan fluorescence is decreased by FRET to pyrene-labeled PE. Titration of 1.5 μM PTEN with mixed POPC/pyrene-PE/anionic lipid(s) vesicles: no anionic lipid ($\diamond$), 5 mol % POPS ($\bullet$), 5 mol % PI-(4,5)P$_2$ ($\triangle$), and 5 mol % POPS with 5 mol % PI(4,5)P$_2$ ($\blacksquare$). Buffer of 150 mM NaCl, 10 mM HEPES, and 0.1 mM EDTA at pH 7.0. All data points were corrected for dilution and the change in Trp fluorescence upon titration in the absence of pyrene-PE. All data points represent the averages of at least three experiments. Solid lines represent best fits using the formalism described in Materials and Methods. ΔF is the initial fluorescence minus the residual fluorescence after a titration step; ΔF_{max} is the maximal fluorescence change observed (normalization).
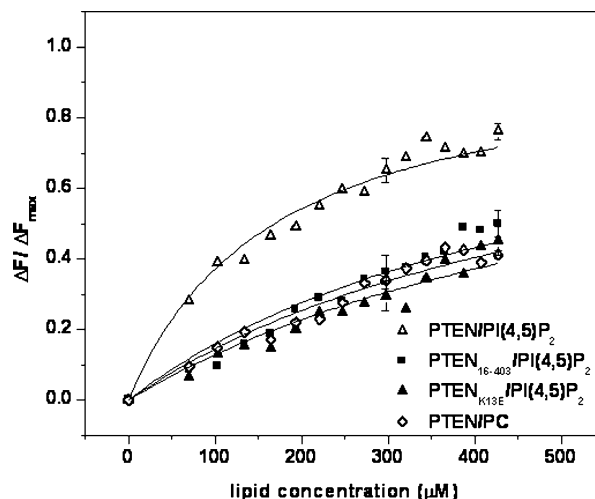

FIGURE 2: Binding of PTEN$_{16-403}$ and PTEN$_{K13E}$. Truncation of PTEN's N-terminus or mutation of the lysine at position 13 abolishes PTEN's ability to bind PI(4,5)P$_2$-containing vesicles. Binding of PTEN$_{K13E}$ ($\blacktriangle$) and PTEN$_{16-403}$ ($\blacksquare$) to PI(4,5)P$_2$ vesicles is similar to binding of full-length PTEN to POPC only vesicles ($\diamond$), highlighting the importance of the lysine at this position. We show data for full-length PTEN binding to PI(4,5)P$_2$-containing vesicles for comparison ($\triangle$). All data points represent the averages of at least three repeats. Solid lines represent best fits using the formalism described in Materials and Methods. Buffer of 150 mM NaCl, 10 mM HEPES, and 0.1 mM EDTA at pH 7.0.

lipid(s) and used only the concentration of the anionic lipid(s) to determine the binding constant. To make the binding constant calculated for anionic lipids easily recognized, we refer to them as K^{PS} or $K^{\text{PI(4,5)P}_2}$.

Infrared Spectroscopy Experiments. FTIR experiments were carried out using a Bruker (Billerica, MA) Tensor spectrometer equipped with a narrow band MCT detector

and a Bruker BioATRII unit. Interferograms were collected at 2 cm^{-1} resolution (512 scans, 20 °C), apodized with a Blackman−Harris function, and Fourier transformed with one level of zero-filling to yield spectra encoded at 1 cm^{-1} intervals. Protein samples were concentrated using 10000 molecular weight cutoff (MWCO) Centricon tubes obtained from Fisher Scientific, reaching a concentration of 8.33 mg/mL. Using Pierce dialysis cartridges with a MWCO of 10000 (Fisher Scientific), protein samples were then exchanged against the D$_2$O buffer described above. Dialysis against buffer was done in three steps, each 20 min in length; 125 μg of the D$_2$O-exchanged protein sample was placed in the ATR unit and analyzed with the Bruker OPUS software. Mixed multilamellar lipid vesicle/protein samples were obtained by resuspending the appropriate lipid mixtures in a protein solution. Collection of IR spectra of this kind does not require the use of unilamellar vesicles. Multilamellar vesicles are ideal for IR data collection because they are formed with protein present in all aqueous compartments, leading to a better signal-to-noise ratio. Lipid samples varied but followed the form 95 mol % POPC, 5 mol % PI(*x,y,z*)-P$_n$, or 90 mol % POPC, 5 mol % POPS, and 5 mol % PI-(4,5)P$_2$. The protein-bearing samples included 1 mol of protein per 8 mol of phosphoinositide lipid. After the protein solution had been added to the dried lipid samples, they were vortexed for 60 s, three times, waiting approximately 5 min between vortexing cycles. The resulting solution of protein and multilamellar vesicles was placed in the BioATR II unit and then analyzed using Bruker OPUS software. The vesicles did not form an anisotropic, ordered film on the ATR crystal but remained isotropic (which was checked by IR measurements using polarized radiation). We obtained buffer spectra by using the buffers against which the proteins had been H$_2$O−D$_2$O exchanged. The D$_2$O buffer samples were adjusted with respect to their H$_2$O (HOD) content so that the intensities of the H$_2$O and HOD bands matched between the respective protein and buffer solutions. Subsequently, the buffer spectra were subtracted from the protein/(lipid) samples to yield a flat baseline between 1600 and 1900 cm^{-1}. All subtraction values were 1.0000 ± 0.0005, indicating an essentially perfect match between buffer and sample spectra. The resulting spectra were exported to Origin software, where the lipid/protein spectra were normalized to the protein only spectrum, using the maximum intensity value of the amide I band (at ≈1638 cm^{-1}). All experiments were repeated at least three times, and representative spectra are shown. The spectra for the repeats are essentially superimposable.

RESULTS

Synergistic Lipid Binding of PTEN. As a first step in assessing the effects of membrane association on PTEN structure, we developed methods for quantifying binding of PTEN to vesicles containing PS, PI(4,5)P$_2$, or both. Interactions of protein with vesicles can be investigated by including small amounts of pyrene- or dansyl-labeled phosphatidylethanolamine (pyrene-PE) in the vesicles (*21, 22*), which reduces Trp fluorescence for proteins bound to these vesicles. Unilamellar vesicles composed of phosphatidylcholine (PC), pyrene-PE, and the anionic lipid of interest were titrated into a PTEN solution, and Trp fluorescence was followed as a function of lipid concentration (Figure 1 and Table 1).

Table 1: Binding Constants for PTEN Binding to Lipid Vesicles with Different Compositions[a]

lipid	K_d (μM), total lipid	K^{lipid} (μM), anionic lipid only
PC	585 ± 15	
PC/PS	508 ± 13	
PC/PI(4,5)P$_2$	163 ± 6	8.14 ± 0.29
PC/PS/PI(4,5)P$_2$	41.4 ± 4.8	2.07 ± 0.24

[a] The binding constants were derived from the fluorescence quenching experiments shown in Figure 1 using the fitting procedure described in Materials and Methods. The total lipid concentration was used to calculate the binding constant (middle column). If the anionic lipid component of the mixed lipid vesicles was primarily responsible for PTEN binding, the binding constant was also derived using only the anionic lipid concentration (right column).

Binding of PTEN to vesicles containing no anionic lipid (PC/pyrene-PE) was similar to that for vesicles with 5 mol % PS (PC/pyrene-PE/PS). This in agreement with earlier findings that only high concentrations of PS substantially enhance PTEN binding (∼3-fold increase in the level of binding for 10 mol % PS) (*17*). In contrast, PC/pyrene-PE/PI(4,5)P$_2$ (5 mol %) vesicles led to an ∼2-fold greater change in Trp fluorescence, indicating that PTEN associates with PI(4,5)P$_2$ more strongly than PS.

To analyze these data, we calculated binding constants by two methods. For all samples, the K_d was calculated using the total lipid concentrations. In addition, for samples in which the binding is dominated by the anionic lipid [PC/PI(4,5)P$_2$ and PC/PI(4,5)P$_2$/PS], we calculated the binding constants using just the concentrations of the anionic lipid(s), which we call $K^{PI(4,5)P_2}$ or $K^{PI(4,5)P_2/PS}$. The observed binding constants in Table 1 are in accord with enzyme kinetic measurements showing that PI(4,5)P$_2$ enhances PI-(3,4,5)P$_3$ hydrolysis more effectively than PS, and the $K^{PI(4,5)P_2}$ of 8.14 μM determined here is in general agreement with the PI(4,5)P$_2$ concentration required to activate the PTEN phosphatase [K_{act} = 20.2 μM (*16*)]. The magnitude of this binding constant indicates that PTEN−PI(4,5)P$_2$ interactions are physiologically relevant since the effective cellular concentration of PI(4,5)P$_2$ is thought to be ∼10 μM, and local PI(4,5)P$_2$ concentrations are likely to reach even higher levels. Increasing the PS concentration to 25 mol % resulted in stronger binding, but even for these higher surface charge densities, K_d was still lower than the corresponding values for the PC/PI(4,5)P$_2$ vesicle system (K_d for 25 mol % PS = 259 ± 20 μM for a total lipid concentration or K^{PS} of 65 ± 5 μM, based on the concentration of the anionic lipid only; titration curve not shown). This observation is in apparent disagreement with earlier findings by Walker et al. (*17*), who reported stronger binding of PTEN to vesicles with 10 mol % PS in comparison to vesicles with 5 mol % PI(4,5)P$_2$.

The main purpose of this set of experiments was to test whether PI(4,5)P$_2$ and PS compete for the same anionic binding site(s) or bind to distinct binding sites and synergistically enhance PTEN binding. We found that PTEN binds to vesicles containing PI(4,5)P$_2$ and PS (both 5 mol %) more effectively than vesicles containing only 5 mol % PI(4,5)P$_2$ or 5 mol % PS (Figure 1). The fit for the PC/PI(4,5)P$_2$PS data is not as good, indicating that binding of PTEN to these more complex lipid systems cannot be adequately described with a simple binding model. Therefore, the binding constant is only an estimate [$K^{PI(4,5)P_2/PS}$ = 2.07 ± 0.24 μM]. To explore whether the enhanced binding to PC/PI(4,5)P$_2$/PS
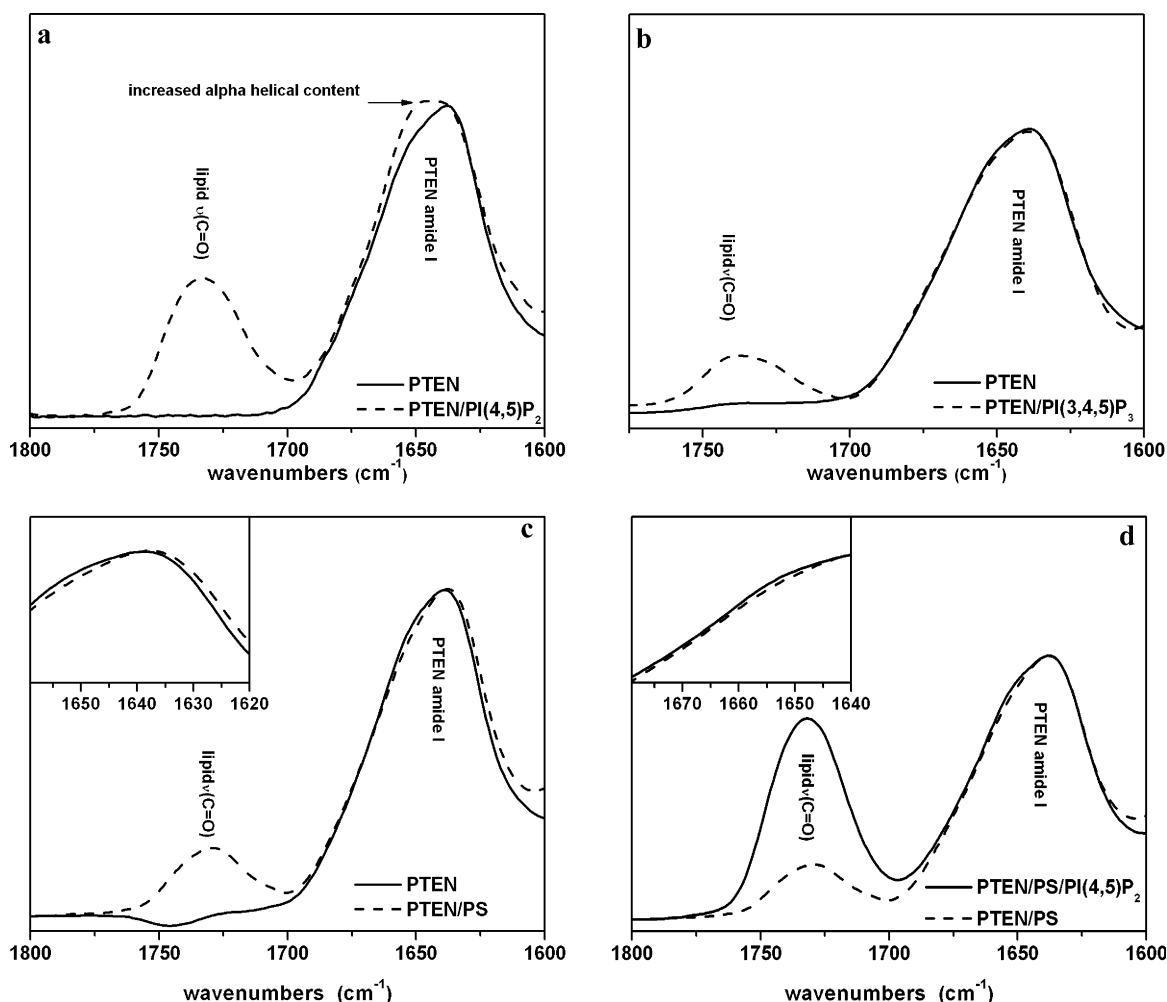
FIGURE 3: Structural changes of PTEN in the presence of PI(4,5)P$_2$- or PI(3,4,5)P$_3$-containing vesicles. Spectra were normalized to amide I peak maximum. Buffer of 150 mM NaCl, 10 mM HEPES, and 0.1 mM EDTA at pH 7.0. (a) Infrared spectra of PTEN in the absence or presence of multilamellar POPC/PI(4,5)P$_2$ mixed vesicles. In the presence of vesicles containing 5 mol % PI(4,5)P$_2$ (- - -), full-length PTEN (—) adopts a more α-helical conformation. (b) Infrared spectra of PTEN were measured in the absence or presence of multilamellar POPC/PI(3,4,5)P$_3$ mixed vesicles. The structure of PTEN (—) does not change in the presence of 5 mol % PI(3,4,5)P$_3$-containing vesicles (- - -). (c) Infrared spectra of PTEN in the absence or presence of multilamellar POPC/PS mixed vesicles. The structure of PTEN (—) shifts toward β-sheet in the presence of 5 mol % POPS-containing vesicles (- - -). (d) Infrared spectra of PTEN in the absence or presence of multilamellar POPC/PS/PI(4,5)P$_2$ mixed vesicles. The spectrum of PTEN in the presence of 5 mol % POPS (- - -) is similar to that in the presence of 5 mol % POPS and 5 mol % PI(4,5)P$_2$ (—). All spectra are representative of at least three experiments. The curves were essentially superimposable.

vesicles is due to the higher surface charge of the vesicles, we assessed binding of PTEN to vesicles that contain 10 mol % PI(4,5)P$_2$, which exhibit a higher surface charge density than the PC/PI(4,5)P$_2$/PS vesicles. Binding of PTEN to these vesicles was weaker than that for the vesicles with both anionic lipids present [$K^{PI(4,5)P_2}$ = 7.2 μM (data not shown)]. These findings suggest that PI(4,5)P$_2$ and PS do not compete for the same binding site and, instead, bind to distinct sites or at least by different mechanisms, enhancing PTEN binding in a synergistic fashion. This point will be addressed further in the Discussion.

We next checked whether this PI(4,5)P$_2$-mediated binding of PTEN is associated with its N-terminal domain. An N-terminally truncated PTEN (amino acids 16−403) has greatly reduced biological activity (9, 16), and PI(4,5)P$_2$ has no effect on binding of PTEN$_{16−403}$ [K_d = 469 ± 13 μM (Figure 2)]. Similarly, the binding of the PTEN mutant K13E, which is a tumor-derived mutation (23, 24) that renders PTEN inactive (17), is not affected by PI(4,5)P$_2$ (K_d = 501 ± 31 μM). Both of these results are consistent with the earlier

suggestions that PTEN's N-terminal domain is the PI(4,5)-P$_2$ interacting module (9, 16).

In summary, the data in Figures 1 and 2 confirm that the enhanced binding of PTEN to PI(4,5)P$_2$-bearing vesicles is associated with its N-terminal domain. In particular, the K13E and PTEN$_{16−403}$ mutant proteins show weakened binding to PI(4,5)P$_2$-containing vesicles. Also, we show that PTEN binds PS and PI(4,5)P$_2$ synergistically. Walker et al. (17) previously suggested that the N-terminal domain might be nonspecific and bind both PS and PI(4,5)P$_2$. However, our binding data indicate that these anionic lipids bind to independent sites.

Lipid-Induced Conformational Changes. Having established that PTEN binds to the lipid vesicles under our experimental conditions, we tested for structural changes in PTEN induced by interactions with membranes containing anionic lipids. Infrared spectroscopy is ideal for these studies because vesicular light scattering does not obscure the spectra, which occurs for CD spectroscopy. Figure 3a compares the infrared spectra of PTEN in the absence and

presence of POPC/PI(4,5)P$_2$ (95:5) mixed multilamellar vesicles. In the presence of PI(4,5)P$_2$, the PTEN amide I band envelope shows a pronounced intensity increase in the spectral region around ≈1654 cm^{-1}. Protein amide I band envelopes are composed of several sub-bands representing the different secondary structure elements of proteins. Band features localized at 1648−1658 cm^{-1} are generally associated with α-helical structures (*25*). This indicates that PTEN, upon interaction with PI(4,5)P$_2$, undergoes a structural change leading to increased α-helical content. In contrast, the presence of PC/PI(3,4,5)P$_3$ mixed vesicles did not lead to changes in PTEN's amide I band envelope (Figure 3b), highlighting the fact that even a highly negatively charged membrane does not affect PTEN's secondary structure in the absence of PI(4,5)P$_2$.

The next question is whether PTEN bound to PS-containing membranes also undergoes a conformational change. Figure 3c shows PTEN's amide I band envelopes in the presence and absence of PS. The presence of PS results in a shift of the amide I band to slightly lower wavenumbers, which is indicative of increased antiparallel β-sheet content (*25*). This observation is not surprising considering that PS binds to the C2 domain, which exhibits predominantly β-sheet structures (*8*). Hence, the anionic lipid, PS, may induce a slight conformational change that is distinct from the PI(4,5)P$_2$ effect.

We compared the spectra for full-length PTEN in the presence of PS and with PS and PI(4,5)P$_2$. In each of three experiments, PI(4,5)P$_2$ in the presence of PS induced only a slight shift to higher wavenumbers (Figure 3d). This apparent difference is much smaller than that observed in the absence of PS (Figure 3a). Because these spectra are complex and the difference is slight, we reserve our detailed interpretation to the Discussion. However, it is clear that PS affects the PI(4,5)P$_2$-induced conformational change in PTEN.

In contrast to full-length PTEN, truncated PTEN$_{16-403}$ did not exhibit any structural changes in the presence of PI(4,5)-P$_2$ (Figure 4a), while the PTEN mutant K13E showed only a very minor increase in α-helical content (Figure 4b). Hence, the PI(4,5)P$_2$-induced changes in PTEN conformation require an intact N-terminal domain.

Specificity of Binding of Lipid to PTEN. It has been suggested that PTEN's N-terminal domain binds anionic lipids via nonspecific electrostatic interactions (*17, 20*). To test whether the phosphorylation pattern on the inositol ring affects phosphoinositide−PTEN interactions, we assessed binding of PTEN to all naturally occurring phosphoinositide derivatives. For this part of the study, we were not able to employ the pyrene-PE binding assay described above because some phosphoinositide derivatives were not commercially available with the needed unsaturated/saturated acyl chain combination. Phosphoinositides with saturated chains form ordered rather than fluid phases, which is likely to affect PTEN−bilayer interactions, particularly if PTEN partially inserts into the bilayer. Instead, we adopted an assay that utilizes large unilamellar vesicles composed of PC and 0.1 mol % chain-labeled BODIPY TMR phosphoinositides (*26*). Binding of peptides or proteins to the phosphoinositides results in lipid clustering and reduced fluorescence due to self-quenching (*27, 28*). Figure 5 shows the reduction in fluorescence for vesicles composed of 99.9% POPC and 0.1 mol % BODIPY TMR-PI(4,5)P$_2$ upon titration with PTEN
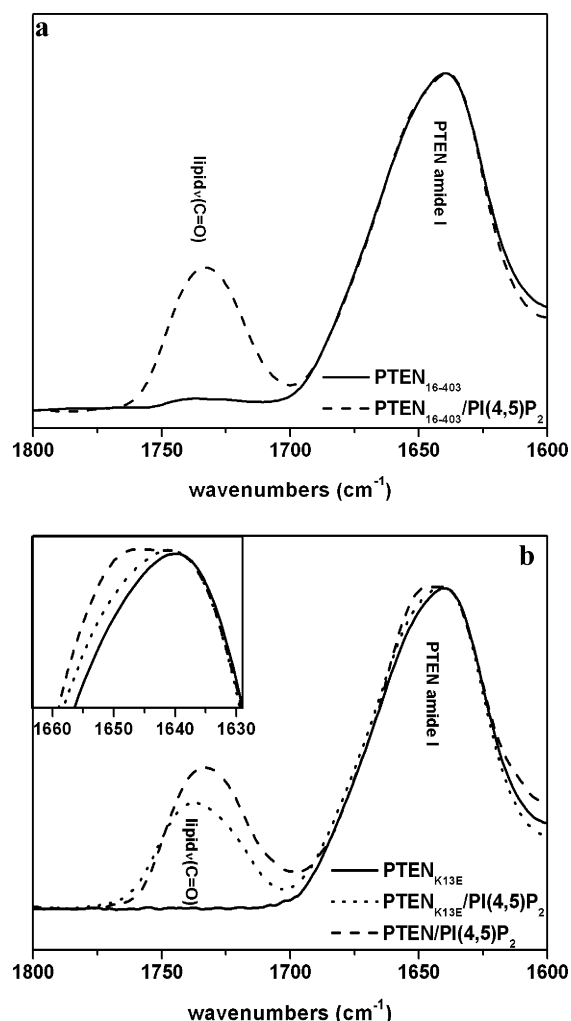

FIGURE 4: Structure of mutated PTEN proteins in the presence of PI(4,5)P$_2$-containing vesicles. Spectra were normalized to amide I peak maximum. Buffer of 150 mM NaCl, 10 mM HEPES, and 0.1 mM EDTA at pH 7.0. (a) Infrared spectra of PTEN$_{16-403}$ in the absence or presence of multilamellar POPC/PI(4,5)P$_2$ mixed vesicles. The structure of PTEN$_{16-403}$ does not change in the presence of 5 mol % PI(4,5)P$_2$ vesicles (- - -). (b) Mutation of the lysine at position 13 of the N-terminus causes a smaller shift toward higher α-helical content. The structure of PTEN$_{K13E}$ (—) is compared to PTEN$_{K13E}$ with vesicles containing 5 mol % PI(4,5)-P$_2$ (···) and PTEN with vesicles containing 5 mol % PI(4,5)P$_2$ (- - -). All presented spectra are representative at least three repeat experiments with essentially superimposable curves.

or the PTEN$_{1-21}$ peptide derived from PTEN's N-terminal sequence. Addition of PTEN or PTEN$_{1-21}$ [PTEN:BODIPY TMR-PI(4,5)P$_2$ maximum molar ratio of 0.5] reduces lipid fluorescence to ∼81 or 91% of its original value, respectively, which is similar to that for other PI(4,5)P$_2$ binding peptides, such as the N-terminal fragment of NAP-22 (neuronal axonal myristoylated membrane protein of 22 kDa) (*29*). Figure 6a summarizes the fluorescence quenching for phosphoinositides [PTEN:BODIPY TMR-PI(x,y,z)P$_n$ ratio of 0.5]. Most strikingly, addition of PTEN to vesicles containing BODIPY TMR-PI(3,4)P$_2$ or BODIPY TMR-PI(3,5)P$_2$ resulted in a reduction in fluorescence intensity 3-fold smaller than that observed for BODIPY TMR-PI(4,5)P$_2$; i.e., PTEN interacts more strongly with PI(4,5)P$_2$ than with the other phosphatidylinositol bisphosphates. Furthermore, even though PI(3,4,5)P$_3$ has a greater negative charge, addition of PTEN to BODIPY TMR-PI(3,4,5)P$_3$ vesicles resulted in a reduction
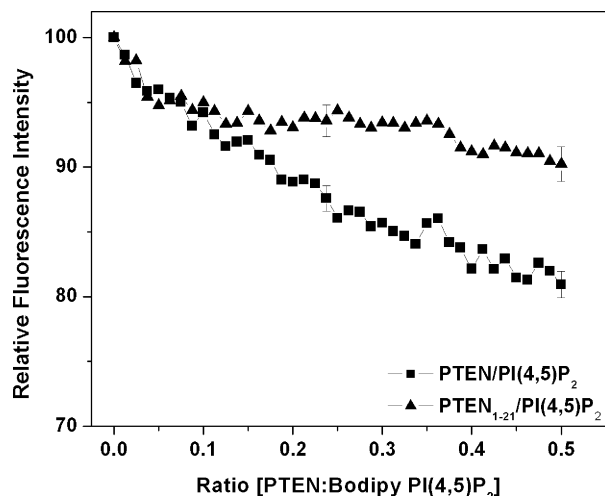
FIGURE 5: Binding of PTEN and PTEN$_{1-21}$ to PI(4,5)P$_2$. Titration of PTEN and peptide PTEN$_{1-21}$ into unilamellar vesicles composed of 99.9 mol % POPC and 0.1 mol % BODIPY TMR-PI(4,5)P$_2$: (■) full-length PTEN and (▲) PTEN$_{1-21}$. All data points represent the averages of at least three repeats. Solid lines represent best fits using the formalism outlined in Materials and Methods.

in fluorescence 6-fold smaller than that observed for BODIPY TMR-PI(4,5)P$_2$. In contrast, PTEN$_{16-403}$ lacks binding specificity for PI(4,5)P$_2$ (Figure 6b). Figure 6c shows that the peptide PTEN$_{1-21}$, which is derived from PTEN's N-terminal end, exhibits slightly weaker binding than full-length PTEN but still shows a preference for PI(4,5)P$_2$. Addition of PTEN$_{1-21}$ to BODIPY TMR-PI(3,4)P$_2$ or BODIPY TMR-PI(3,5)P$_2$ vesicles resulted in a reduction in fluorescence ∼2-fold smaller than that observed for BODIPY TMR-PI(4,5)P$_2$. These binding preferences mirror the previously observed activation of PTEN phosphatase by PI(4,5)-P$_2$ (*16*) and the assignment of the N-terminal region as the PI(4,5)P$_2$-binding domain.

To further test the specificity of the PTEN−phosphoinositide interaction, we characterized PTEN's secondary structure in the presence of PI(3,5)P$_2$ (Figure 7). PI(3,5)P$_2$ did not alter PTEN's secondary structure, consistent with the weak binding of PTEN to PI(3,5)P$_2$ (Figure 6a).

To determine whether the increased α-helical content observed for full-length PTEN in the presence of PI(4,5)P$_2$ is localized in the N-terminal domain, we conducted circular dichroism (CD) and IR experiments on the peptide PTEN$_{1-21}$, i.e., PTEN's N-terminal domain that includes the PI(4,5)-P$_2$-binding domain. The CD measurements [PI(4,5)P$_2$ micelles] and IR experiments [POPC/PI(4,5)P$_2$ mixed vesicles] did not reveal any structural changes in peptide PTEN$_{1-21}$; i.e., the peptide remained in an apparently random conformation upon interaction with PI(4,5)P$_2$ (data not shown). Although there is some risk in deducing structures of protein segments from peptide studies, it seems to be a reasonable approach in this case because the full-length PTEN and the N-terminal peptide have similar phosphoinositide binding preferences (Figure 6).

DISCUSSION

The major conclusions from this study follow. (1) The N-terminal domain preferentially binds PI(4,5)P$_2$. (2) Binding of PI(4,5)P$_2$ induces a conformational change resulting in increased α-helical content. Association of PTEN to PC/PS

vesicles is not sufficient to induce this conformational change. (3) Despite its inability to induce the α-helical conformational change, PS does enhance binding of PTEN to PI(4,5)P$_2$-containing vesicles, indicating that these anionic lipids bind to independent sites. These results strongly support our proposal that PI(4,5)P$_2$ regulates PTEN conformation by an allosteric mechanism and provide the first evidence that the conformational change occurs in the phosphatase domain. This regulation is important since there are a number of cancer-related point mutations in the N-terminal PI(4,5)P$_2$-binding domain, and truncated PTEN proteins lacking the PI(4,5)P$_2$-binding domain show greatly reduced membrane binding and biological activity. The PI-(4,5)P$_2$-induced conformational change is one of the mechanisms by which PTEN phosphatase activity is maintained at correct levels, which is essential for suppressing carcinogenesis.

Using several independent approaches, we have demonstrated a specific interaction between PTEN and PI(4,5)P$_2$. We have shown saturable binding of PTEN to PI(4,5)P$_2$-containing vesicles. In addition, we assessed binding for all natural phosphoinositides and detected preferential binding for PI(4,5)P$_2$, which is intriguing since this lipid activates PTEN (*16*). The K13E PTEN mutant and the truncated PTEN$_{16-403}$ show greatly weakened binding to PI(4,5)P$_2$-containing vesicles. Finally, a PTEN$_{1-21}$ peptide also showed preferential binding to PI(4,5)P$_2$.

What is the origin of this specificity for PI(4,5)P$_2$? The sequence of the PTEN PI(4,5)P$_2$-binding domain is in general agreement with the signature binding motif for PI(4,5)P$_2$-binding domains, such as gelsolin (*30, 31*). PTEN's N-terminal domain has been compared to MARCKS$_{151-175}$ (myristoylated alanine-rich C-kinase substrate), which has been reported to have a nonspecific electrostatic interaction with PI(4,5)P$_2$ (*28*). On the basis of this observation, it has been proposed that PTEN also binds to PI(4,5)P$_2$ via nonspecific electrostatic interactions (*20*). However, in this study, we demonstrate that PTEN discriminates between different phosphoinositides with the same net charge. Furthermore, PI(3,4,5)P$_3$, the phosphoinositide with the greatest negative charge, does not enhance binding of PTEN to vesicles and does not activate PTEN phosphatase activity (*9, 16*). Finally, the K13E PTEN mutant showed greatly weakened binding to PI(4,5)P$_2$ vesicles, even though the N-terminus of this mutant PTEN still contains a large number of positively charged amino acids. Small protein segments or peptides for phosphoinositides also have been shown to specifically bind phosphoinositides. For example, the N-terminal fragment of NAP-22 peptide binds more strongly to PI(4,5)P$_2$ vesicles than to PI(3,5)P$_2$ vesicles (*29*). In this study, we observed that the PTEN$_{1-21}$ peptide preferentially binds PI(4,5)P$_2$. Both peptides (PTEN$_{1-21}$ and NAP-22) exhibit behavior different from that of the MARCKS peptide that lacks phosphoinositide specificity. The MARCKS peptide is very highly positively charged (13 of 25 amino acids), whereas our PTEN$_{1-21}$ peptide has five positively charged amino acids out of 21. A plausible explanation is that the MARCKS peptide is so highly charged that it binds anionic lipids nonspecifically, but less positively charged peptides, such as PTEN$_{1-21}$, require both nonspecific electrostatic and specific interactions for strong binding. Therefore, hydrogen bonds are likely to be important for the interaction of PTEN's
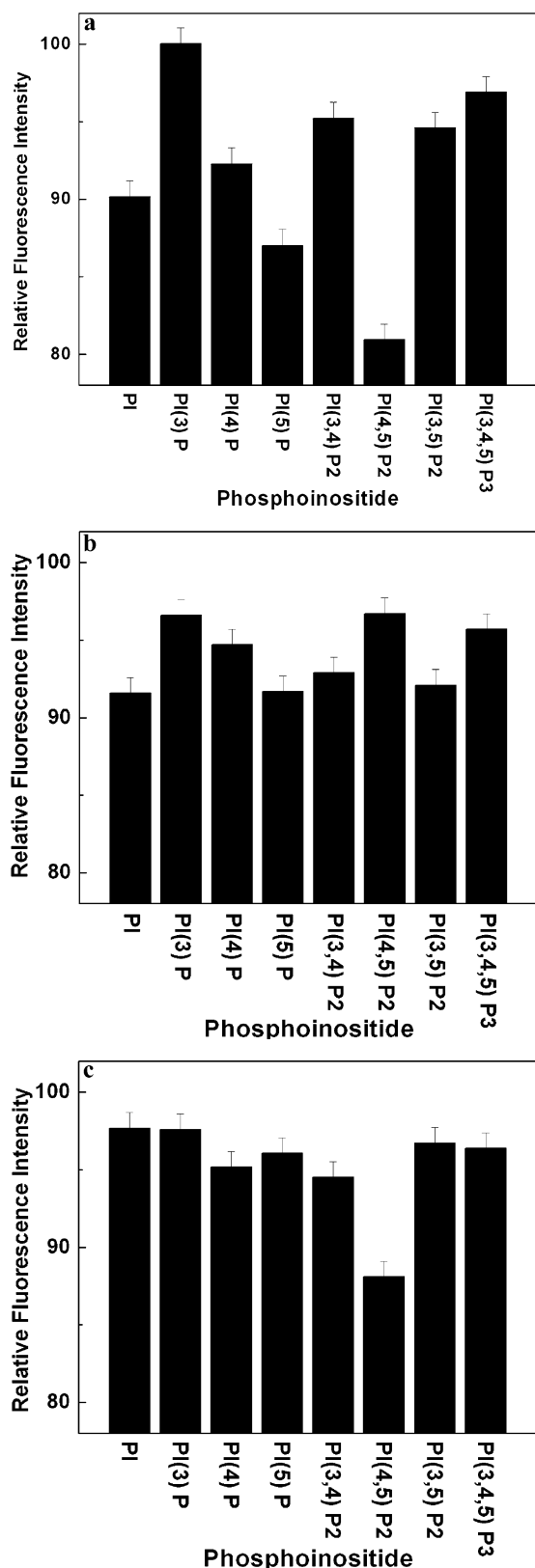
FIGURE 6: Binding specificities of PTEN, $PTEN_{16-403}$, and $PTEN_{1-21}$ for unilamellar vesicles composed of 99.9% POPC and 0.1% BODIPY TMR-PI(x,y,z)P$_n$. The quenching at the highest lipid concentration is given (see Figure 5 for details). Each bar represents the average of at least three independent titrations. The error bar represents the maximum deviation from the average value. (a) Full-length PTEN shows specific binding, preferring PI(4,5)P$_2$ over other phosphoinositides. (b) $PTEN_{16-403}$, lacking PTEN's N-terminus, does not show a preference for PI(4,5)P$_2$. (c) The N-terminal peptide, $PTEN_{1-21}$, also shows a preference for PI(4,5)P$_2$.
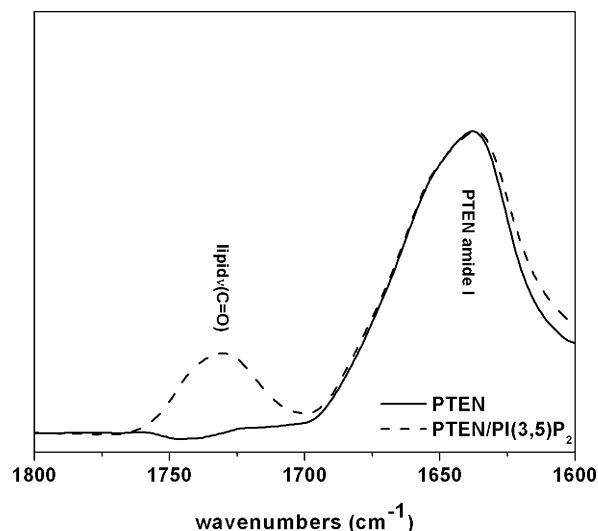

FIGURE 7: Structure of PTEN in the presence of PI(3,5)P$_2$-containing vesicles. Spectra were normalized to the amide I peak maximum. Buffer of 150 mM NaCl, 10 mM HEPES, and 0.1 mM EDTA (pH 7.0). Infrared spectra of PTEN were measured in the absence or presence of multilamellar POPC/PI(3,5)P$_2$ mixed vesicles. The structure of PTEN (—) does not change in the presence of vesicles containing PI(3,5)P$_2$ (- - -).

N-terminal end with phosphoinositides, and it appears that optimal interaction requires a specific orientation and/or sequence of the functional groups at the phosphoinositide inositol ring, leading to the preferential binding of PTEN to PI(4,5)P$_2$.

A critical question is which PTEN domain(s) undergoes the structural change with increased α-helical content. The phosphatase domain is largely α-helical and is a good candidate. This hypothesis is supported by preliminary fluorescence studies on PTEN Trp 111 in the phosphatase domain (not shown). In addition, although the N-terminus is a PI(4,5)P$_2$-binding domain and $PTEN_{1-21}$ preferentially binds PI(4,5)P$_2$, we were unable to detect any change in secondary structure for the N-terminal peptide. The peptide exhibits the same binding preference as PTEN; i.e., the peptide conformation is likely to be the same as the secondary structure of the corresponding N-terminal end of PTEN. Hence, we do not think that the shift in the infrared spectrum for full-length PTEN reflects changes in the residues directly interacting with PI(4,5)P$_2$. PI(4,5)P$_2$ did not induce an obvious change in the amide sub-band associated with the β-sheet. Because the C2 domain is largely β-sheet, there do not appear to be PI(4,5)P$_2$-induced changes in the C2 domain. The simplest interpretation of these data is that PI(4,5)P$_2$ enhances the α-helical content of the phosphatase domain.

A natural question is whether the fraction of bound PTEN affects the interpretation of the infrared spectra. For example, PS does not induce an increase in α-helicity. Our interpretation is that PS does not induce the same conformational change that PI(4,5)P$_2$ does. However, one might ask whether the inability to detect increased α-helical structure is due to a smaller percentage of PTEN bound to PS vesicles. We reject the second interpretation for two reasons. First, vesicles with high PS concentrations that bind as much PTEN as PI-(4,5)P$_2$ do not increase α-helical content. Second, we are using ATR cells to measure the infrared spectra. In initial experiments, we noted that the protein infrared spectra were

less intense for PTEN mutants with a decreased level of membrane association. This was a result of large multilamellar vesicles settling on top of the ATR crystal. Because the ATR crystal detects absorbance only within a few micrometers of the crystal, this system preferentially detects membrane-bound protein. As a result, the infrared absorbance spectra emphasize membrane-bound PTEN and are not obscured by soluble PTEN.

PS at high concentrations (10 mol %) can enhance binding of PTEN to vesicles, and 5 mol % can enhance binding to $PI(4,5)P_2$-containing vesicles. This result suggests that PTEN binds $PI(4,5)P_2$ and PS at separate sites. Indeed, it is common for interfacial enzymes to bind to membranes via multiple sites (*32*). On the flip side, Das et al. (*11*) found binding of PTEN to PC/PS and PC/PG vesicles to be essentially the same, implying that PTEN's interaction with PS is the result of nonspecific long-range electrostatic interactions. Combining our findings with those of Das et al. leads to a model in which PTEN is initially attracted by the $PS/PI(4,5)P_2$ electric double layer and subsequently binds specifically to $PI(4,5)P_2$. In the context of such a model, however, it is unclear why PTEN exhibits a weaker binding to vesicles with 10 mol % $PI(4,5)P_2$ than to the less charged PC/PS (5 mol %)/$PI(4,5)P_2$ (5 mol %) vesicles. It might be that the observed binding preference for vesicles containing both PS and $PI(4,5)P_2$ is the result of an altered lateral organization and/or a different protonation state of $PI(4,5)P_2$ in the presence of PS. But it might also well be that PTEN binds to both PS and PG via specific hydrogen bond formation rather than though nonspecific long-range electrostatic interactions. This data set does not allow us to decide unequivocally whether association of PS with PTEN occurs via a specific binding site, long-range electrostatic nonspecific interactions, or both of these mechanisms.

For PTEN bound to PS vesicles, there was a slight shift of the amide band to the β-sheet region of the spectrum, but it is difficult to judge the significance of this slight shift. We also assessed the effects of PS on the $PI(4,5)P_2$-induced increase in α-helical content (Figure 3d). PS reduced the amide band shift caused by $PI(4,5)P_2$. However, we have to interpret this result with caution. The amide band is a sum of peaks for α-helix, β-sheet, β-turn, and random coil. It is difficult to deconvolute the spectra into these individual components, and we cannot say whether one of these other components shifted, causing an apparent decrease in α-helical content. Hence, we cannot state for certain whether PTEN associated with $PI(4,5)P_2$/PS vesicles assumes a distinct conformation or a conformation that includes the $PI(4,5)P_2$-induced changes in the phosphatase domain and the PS-induced changes in the C2 domain.

The data obtained in this study are in agreement with the model developed by Downes and co-workers (*9, 17*), which suggested that membrane association is crucial for full PTEN activity and function. In addition to aiding PTEN's membrane association, we propose that $PI(4,5)P_2$ induces the phosphatase domain to undergo a conformational change, resulting in enhanced phosphatase activity. There are precedents for such regulation in other phosphatases (*33–35*). Phosphatases assume open and closed conformations by movement of the P or WPD loops at the active site. For the substrate to bind, the loop has to be in the open position. For hydrolysis of the substrate, the loop has to close. If the

phosphatase cannot cycle between open and closed conformations, then phosphatase activity is inhibited. Cycling for protein tyrosine phosphatase 1B can be allosterically regulated (*34*). Even though such open and closed states have not been demonstrated for PTEN, this is still an appealing model. We plan to test further whether $PI(4,5)P_2$ binding affects cycling between open and closed states.

ACKNOWLEDGMENT

REFERENCES

1. Maehama, T., and Dixon, J. E. (1998) The tumor suppressor, PTEN/MMAC1, dephosphorylates the lipid second messenger, phosphatidylinositol 3,4,5-trisphosphate, *J. Biol. Chem. 273*, 13375–13378.
2. Leslie, N. R., and Downes, C. P. (2004) PTEN function: How normal cells control it and tumour cells lose it, *Biochem. J. 382*, 1–11.
3. Datta, S. R., Brunet, A., and Greeberg, M. E. (1999) Cellular survival: A play in three Akts, *Genes Dev. 13*, 2905–2927.
4. Stocker, H., Andjelkovic, M., Oldham, S., Laffargue, M., Wymann, M. P., Hemings, B. A., and Hafen, E. (2002) Living with lethal PIP3 levels: Viability of flies lacking PTEN restored by a PH domain mutation in Akt/PKB, *Science 295*, 2088–2091.
5. Stiles, B., Groszer, M., Wang, S., Jiao, J., and Wu, H. (2004) PTEN: Less means more, *Dev. Biol. 273*, 175–184.
6. Sansal, I., and Seller, W. R. (2004) The biology and clinical relevance of the PTEN tumor suppressor pathway, *J. Clin. Oncol. 22*, 2954–2963.
7. Simpson, L., and Parsons, R. (2001) PTEN: Life as a tumor suppressor, *Exp. Cell Res. 264*, 29–41.
8. Lee, J. O., Yang, H. J., Gerogescu, M. M., Di Cristofano, A., Maehama, T., Shi, Y. G., Dixon, J. E., Pandolfi, P., and Pavletich, N. P. (1999) Crystal structure of the PTEN tumor suppressor: Implications for its phosphoinositide phosphatase activity and membrane association, *Cell 99*, 323–334.
9. McConnachie, G., Pass, I., Walker, S. M., and Downes, C. P. (2003) Interfacial kinetic analysis of the tumour suppressor phosphatase, PTEN: Evidence for activation by anionic phospholipids, *Biochem. J. 371*, 947–955.
10. Vazquez, F., Matsuoka, S., Sellers, W. R., Yanagida, T., Ueda, M., and Devreotes, P. N. (2006) Tumor suppressor PTEN acts through dynamic interaction with the plasma membrane, *Proc. Natl. Acad. Sci. U.S.A. 103*, 3633–3638.
11. Das, S., Dixon, J. E., and Cho, W. W. (2003) Membrane-binding and activation mechanism of PTEN, *Proc. Natl. Acad. Sci. U.S.A. 100*, 7491–7496.
12. Vazquez, F., and Devreotes, P. N. (2006) Regulation of PTEN function as a PIP3 gatekeeper through membrane interaction, *Cell Cycle 5*, 1523–1527.
13. Toner, M., Vaio, G., McLaughlin, A., and McLaughlin, S. (1988) Adsorption of cations to phosphatidylinositol-4,5-bisphosphate, *Biochemistry 27*, 7435–7443.
14. Redfern, D. A., and Gericke, A. (2005) pH dependent microdomain formation in phosphatidylinositol polyphosphate/phosphatidylcholine mixed vesicles, *J. Lipid Res. 46*, 504–515.
15. Redfern, D. A., and Gericke, A. (2004) Domain formation in phosphatidylinositol monophosphate/phosphatidylcholine model membrane systems, *Biophys. J. 86*, 2980–2992.
16. Campbell, R. B., Liu, F. H., and Ross, A. H. (2003) Allosteric activation of PTEN phosphatase by phosphatidylinositol 4,5-bisphosphate, *J. Biol. Chem. 278*, 33617–33620.
17. Walker, S. M., Leslie, N. R., Perera, N. M., Batty, I. H., and Downes, C. P. (2004) The tumour suppressor function of PTEN requires an N-terminal lipid binding motif, *Biochem. J. 379*, 301–307.
18. Iijima, M., Huang, Y. E., Luo, H. R., Vazquez, F., and Devreotes, P. N. (2004) Novel mechanism of PTEN regulation by its phosphatidylinositol 4,5-bisphosphate binding motif is critical for chemotaxis, *J. Biol. Chem. 279*, 16606–16613.
19. Schaletzky, J., Dove, S. K., Short, B., Lorenzo, O., Clague, M. J., and Barr, F. A. (2003) Phosphatidylinositol-5-phosphate activation

and conserved substrate specificity of the myotubularin phosphatidylinositol 3-phosphatases, *Curr. Biol. 13*, 504−509.

20. Mulgrew-Nesbitt, A., Diraviyam, K., Wang, J., Singh, S., Murray, P., Li, Z., Rogers, L., Mirkovic, N., and Murray, D. (2006) The role of electrostatics in protein-membrane interactions, *Biochim. Biophys. Acta 1761*, 812−826.

21. Evans, J. H., Murray, D., Leslie, C. C., and Falke, J. J. (2006) Specific translocation of protein kinase Cα to the plasma membrane requires both Ca^{2+} and PIP_2 recognition by its C2 domain, *Mol. Biol. Cell 17*, 56−66.

22. Tatulian, S. A., Qin, S., Pande, A. H., and He, X. E. (2005) Positioning membrane proteins by novel protein engineering and biophysical approaches, *J. Mol. Biol. 351*, 939−947.

23. Gronback, K., Zeuthen, J., Guldberg, P., Ralfkiaer, E., and Hou-Jensen, K. (1998) Alterations of the MMAC1/PTEN gene in lymphoid malignanicies, *Blood 91*, 4388−4390.

24. Yokoyama, Y., Wan, X., Shinohara, A., Takahashi, Y., Niwa, K., and Tamaya, T. (2000) Expression of PTEN and PTEN pseudogene in endometrial carcinoma, *Int. J. Mol. Med. 6*, 47−50.

25. Arrondo, J. L. R., and Goni, F. M. (1999) Structure and dynamics of membrane proteins as studied by infrared spectroscopy, *Prog. Biophys. Mol. Biol. 72*, 367−405.

26. Gambhir, A., Hangyas-Mihalye, G., Zaitseva, I., Cafiso, D. S., Wang, J., Murray, D., Pentyala, S. N., Smith, S. O., and McLaughlin, S. (2004) Electrostatic sequestration of PIP2 on phospholipid membranes by basic/aromatic regions of proteins, *Biophys. J. 86*, 2188−2207.

27. Wang, J., Arbuzova, G., Hangyas-Mihalye, G., and McLaughlin, S. (2001) The effector domain of myristoylated alanine-rich C-kinase substrate (MARCKS) binds strongly to phosphatidylinositol 4,5-bisphosphate (PIP2), *J. Biol. Chem. 276*, 5012.

28. Wang, J., Gambhir, A., Hangyas-Mihalye, G., and McLaughlin, S. (2002) Lateral sequestration of phosphatidylinositol 4,5-bisphosphate by the basic effector domain of myristoylated alanine-rich C-kinase substrate is due to non-specific electrostatic interactions, *J. Biol. Chem. 277*, 34401.

29. Epand, R. M., Vuong, P., Yip, C. M., Maekawa, S., and Epand, R. F. (2004) Cholesterol-dependent partitioning of Ptdlns(4,5)P-2 into membrane domains by the N-terminal fragment of NAP-22 (neuronal axonal myristoylated membrane protein of 22 kDa), *Biochem. J. 379*, 527−532.

30. Martin, T. F. J. (1998) Phosphoinositide lipids as signaling molecules: Common themes for signal transduction, cytoskeletal regulation, and membrane trafficking, *Annu. Rev. Cell Dev. Biol. 14*, 231−264.

31. Yin, H. L., and Janmey, P. A. (2003) Phosphoinositide regulation of the actin cytoskeleton, *Annu. Rev. Phys. 65*, 761−789.

32. Jain, M. K., and Berg, O. G. (2006) Coupling of the i-face and the active site of phospholipase A2 for interfacial activation, *Curr. Opin. Chem. Biol. 10*, 473−479.

33. Khajehpour, M., Wu, L., Liu, S. J., Zhadin, N., Zhang, Z. Y., and Callender, R. (2007) Loop dynamics and ligand binding kinetics in the reaction catalyzed by the *Yersinia* protein tyrosine phosphatase, *Biochemistry 46*, 4370−4378.

34. Wiesmann, C., Barr, K. J., Kung, J., Zhu, J., Erlanson, D. A., Shen, W., Fahr, B. J., Zhing, M., Taylor, L., Randal, M., McDowell, R. S., and Hansen, S. K. (2004) Allosteric inhibition of protein tyrosine phosphatase 1B, *Nat. Struct. Mol. Biol. 11*, 730−737.

35. Puhl, A. A., Gruninger, R. J., Greiner, R., Janzen, T. W., Mosimann, S. C., and Selinger, L. B. (2007) Kinetic and structural analysis of a bacterial protein tyrosine phosphatase-like myo-inositol polyphosphatase, *Protein Sci. 16*, 1368−1378.